

# Tolerancing microlenses using ZEMAX<sup>®</sup>

Andrew Stockham, John G. Smith  
MEMS Optical\*, Inc., 205 Import Circle, Huntsville, AL, USA 35806

## ABSTRACT

This paper demonstrates a new tolerancing technique that allows the prediction of microlens optical performance based on metrology measurements taken during the fabrication process. A method for tolerancing microlenses to ensure operating performance using the optical design code ZEMAX<sup>®</sup> is presented. Parameters able to be measured by available metrology tools are assigned tolerances. The goal of the tolerance analysis is to assess the sensitivity of a microlens design to changes in the shape of the lens surface with regard to specific optical performance criteria related to the intended application. Two designs are presented with the tolerance analysis results. In the first design, the radius of curvature and conic constant are varied for an aspheric lens, and the change in the spot size is determined. For the second design, fiber-coupling efficiency is tabulated for a biconic lens. In each case, a metric can be produced showing the ability of the design to meet performance goals within the specified tolerances. A fabrication technician can then use this tolerancing metric with appropriate metrology data to determine if the device will yield acceptable performance. The metric can also determine if a design is overly sensitive to expected tolerances, thereby allowing the optical designer to evaluate the design from a manufacturing perspective.

**Keywords:** Manufacturing tolerances, ZEMAX<sup>®</sup>, microlenses, aspheric lenses, micro-optics, metrology, grayscale lithography

## 1. INTRODUCTION

The design and manufacture of lenses has always been more of an art than a science.<sup>1</sup> Even today, with the aid of optical design codes such as ZEMAX<sup>®</sup>, the process of designing and analyzing a lens for manufacturing tolerances remains highly subjective. A typical design process often begins with the designer selecting a lens that has already been invented—the designer using his or her experience to pick a lens with performance nearest to the requirements. Likewise, lens manufacturers continue to grind and polish lenses to this day. Since only a small amount of the surface is removed with each polish cycle, the accuracy of the lens shape can be continuously verified during its manufacture. Current tolerance techniques implicitly assume this method of manufacturing; however, the general method of microlens fabrication uses wafer-scale processing, which does not permit iterative fabrication. Therefore, it is the opinion of the authors of this paper that a new tolerance technique is needed.

A microlens is by definition any lens of small size, typically less than 2mm in diameter. In most cases, such a small lens would be too difficult to handle and too costly to manufacture individually. When fabricating microlenses using wafer-scale processing, it is no longer practical to polish an individual lens, as there may be thousands of such lenses on a wafer. In addition, each lens may be slightly different than its neighbors. Consequently, one must be familiar with the uniformity of the fabrication process. If only the minimum, maximum, and nominal values for each tolerance are used in the tolerance analysis, the design space will be severely under sampled. Not to mention that such an analysis will only track the performance for one parameter at a time, telling the designer nothing about how the parameters depend on one another. In order to fill in the design space completely, it is necessary to run a large number of tolerance analyses and tabulate the results. This can be done very easily in ZEMAX<sup>®</sup> using the Monte Carlo method in the tolerance analysis along with a tolerance script. A quick glance at a plot of the results, and one can begin to evaluate the sensitivity of the design. It will also tie the design parameters that can be measured with available metrology tools, such as radius of curvature and conic constant, into optical performance parameters, such as spot size or coupling efficiency.

---

\* info@memsoptical.com; phone 1 256 859-1886; fax 1 256 859-5890; www.memsoptical.com

Copyright 2006 Society of Photo-Optical Instrumentation Engineers. This paper will be published in SPIE Proceedings Micromachining and Technology for Micro-Optics and Nano-Optics IV and is made available as an electronic preprint with permission of SPIE. One print or electronic copy may be made for personal use only. Systematic or multiple reproduction, distribution to multiple locations via electronic or other means, duplication of any material in this paper for a fee or for commercial purposes, or modification of the content of the paper are prohibited.

During fabrication, the design parameters can be measured and plotted on a graph overlaying the results of the tolerance analysis, immediately indicating to the technician whether the lens will provide good performance.

## 2. GRAYSCALE TECHNOLOGY OVERVIEW

Grayscale technology provides a fabrication flexibility that far exceeds that of binary technology. This is particularly apparent in fabricating refractive microlenses, surfaces that are both refractive and diffractive, and exotic dual focus or color separation devices. Such elements might require several hundred different gray levels and fabricating these with binary chrome masks would be impractical.

The fabrication of such a complex surface relief structure is enabled by the use of grayscale technology. Grayscale photolithography uses a photomask that has a spatially varying transmission. As a result, the amount of energy that is allowed through the mask varies as a function of position as shown in Figure 1. This additional dimension of freedom in the lithography step allows for the realization of complex three-dimensional structures such as aspheric lenses.

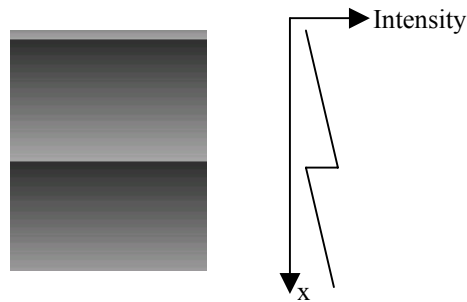


Fig. 1. Illustration of the variable transmission of a grayscale photomask.

The grayscale photomask is then used to partially expose photoresist as shown in Figure 2. After photolithography is complete, an etching process is used to transfer the shape into the substrate (the shaded region). The height of the final structure in the substrate is controlled by the ratio of the etch rate of the substrate to the etch rate of the photoresist, defined as the selectivity,

$$S \equiv \frac{R_S}{R_{PR}}. \quad (1)$$

Thus, the final height of the structure is the product of the photoresist height with the selectivity:

$$H_S = S H_{PR}. \quad (2)$$

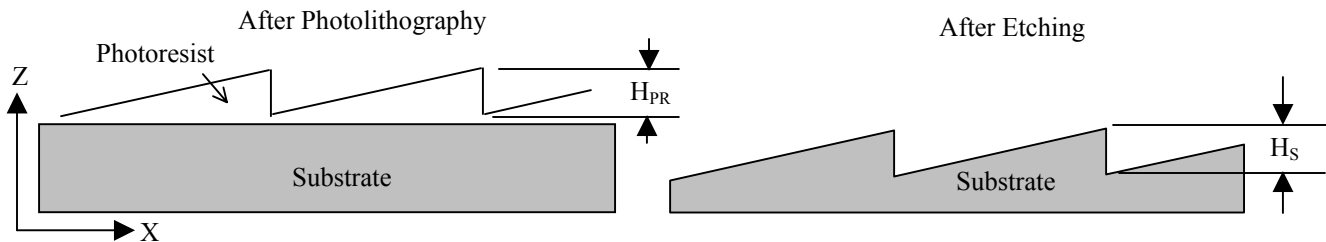


Fig. 2. Side profile of the result of a grayscale lithography and etching process.

Copyright 2006 Society of Photo-Optical Instrumentation Engineers. This paper will be published in SPIE Proceedings Micromachining and Technology for Micro-Optics and Nano-Optics IV and is made available as an electronic preprint with permission of SPIE. One print or electronic copy may be made for personal use only. Systematic or multiple reproduction, distribution to multiple locations via electronic or other means, duplication of any material in this paper for a fee or for commercial purposes, or modification of the content of the paper are prohibited.

Grayscale lithography is a wafer-scale process in which a single die is stepped and repeated across a wafer. Uniformity of the etch across a wafer is generally 3-5%,<sup>2,3</sup> although this could be improved through process refinements. This means that even if the die was assumed to be perfect and the pattern transferred faithfully into the photoresist, the etch depth of all the dies will fall within a specified range. If the die is a lens, this results in a different sag and different radius of curvature and conic value for each lens. During reactive plasma etching of grayscale features, the etch selectivity varies as a function of the amount of photoresist exposed. If the selectivity were to decrease, the lens would tend to flatten out near the apex, producing a shape similar to that of a lens with a larger radius of curvature but a more positive conic constant. Similarly, if the selectivity were to increase, the lens would appear flatter toward the bottom, which is characteristic of a lens with a more negative conic constant.

Based on the manufacturability of microlenses using grayscale technology, there are several parameters that can have tolerances: sag of the lens, refractive index of the substrate material, wafer thickness, and element tilt and decenter. It will be assumed for the following analysis that changes in the refractive index of the substrate material and wafer thickness are small enough that they can safely be ignored. Furthermore, placing tolerances on element tilt and decenter requires knowledge of how the device will be assembled and is outside the scope of this paper. In addition, two assumptions are made about grayscale technology in order to tolerance microlenses: only the etch depth (or sag) matters, and the etch uniformity varies randomly. For a lens, the sag is a function of radius of curvature and conic constant. The conic equation for a lens can be expressed as

$$r^2 - 2Rz + (k + 1)z^2 = 0, \quad (3)$$

where  $R$  is the radius of curvature,  $k$  is the conic constant, and  $z$  is the sag of the lens at radial position  $r$ . Solving for  $z$  yields a more familiar expression for the sag of a lens

$$z = \frac{r^2/R}{1 + \sqrt{1 - [(k + 1)r^2/R^2]}}. \quad (4)$$

We will want to know what change is required in the design variables  $R$  and  $k$ , to affect a predetermined change in  $z$ . To do this we must first solve equation 3 in terms of  $R$  and  $k$ , respectively:

$$R(z) = \frac{r^2}{2z} + \frac{1}{2}(k + 1)z, \quad (5)$$

and

$$k(z) = -\frac{r^2}{z^2} + \frac{2R}{z} - 1. \quad (6)$$

Next, differentiating equations 5 and 6 with respect to  $z$  gives:

$$\frac{\partial R}{\partial z} = -\frac{r^2}{2z^2} + \frac{1}{2}(k + 1), \quad (7)$$

and

$$\frac{\partial k}{\partial z} = \frac{2r^2}{z^3} - \frac{2R}{z^2}. \quad (8)$$

Equations 7 and 8 will provide the tolerance range for radius of curvature and conic constant, respectively, as will be shown in greater detail below.

Copyright 2006 Society of Photo-Optical Instrumentation Engineers. This paper will be published in SPIE Proceedings Micromachining and Technology for Micro-Optics and Nano-Optics IV and is made available as an electronic preprint with permission of SPIE. One print or electronic copy may be made for personal use only. Systematic or multiple reproduction, distribution to multiple locations via electronic or other means, duplication of any material in this paper for a fee or for commercial purposes, or modification of the content of the paper are prohibited.

### 3. INCREASING FILL FACTOR ON DETECTOR ARRAYS

Photodiode (CMOS) detectors have the advantage of being faster than CCD detectors but with lower fill factors. Microlens arrays are commonly used to increase the fill factor of the detector by focusing more light onto the active area. An avalanche photodiode (APD) is a variation of a  $p-n$  junction photodiode. When biased beyond its breakdown voltage, an APD is capable of detecting single photons. In this mode, called "Geiger mode", an incident photon absorbed by the active area could potentially produce a detectable current pulse with rise times of a nanosecond or better and durations of 10-20 ns.<sup>4</sup> Additionally, this pulse can trigger a CMOS circuit integrated into the pixel. Single-photon sensitivity can be realized with sub-nanosecond precision. Integrated APD/CMOS arrays make possible a compact, low-power, all-solid-state sensor.<sup>5</sup> The speed and sensitivity of the detector is limited by its bias voltage and dark current, respectively. Smaller devices are more sensitive because the dark current is proportional to the size of the active area. Crosstalk is an additional complication that is best reduced by increasing the distance between the pixels. Unfortunately, this combination results in very low fill factor arrays.

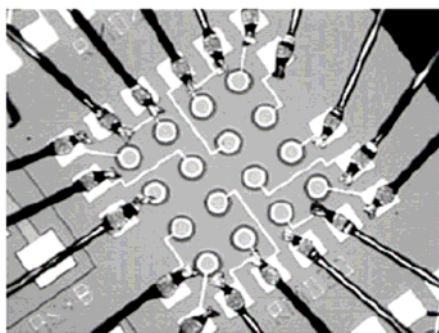


Fig. 3. Avalanche photodiode array produced by a government sponsored laboratory. The individual elements are the circular pads 30  $\mu\text{m}$  in diameter, separated by 100  $\mu\text{m}$  in each dimension.<sup>4</sup>

Let us design a microlens array for a hypothetical APD array that has an active area of 10  $\mu\text{m}$  and a pixel pitch of 250  $\mu\text{m}$ . Let us further assume that these are InGaAs detectors on an InP substrate for an operating wavelength of 1064 nm. We will need a material that transmits at this wavelength. Gallium phosphide (GaP) is a good choice, as it has similar refractive index to InP and can be bonded to it for back-illumination with low reflection losses at the interface. We will assume the GaP wafer has a standard thickness of 300  $\mu\text{m}$ . In order to simplify matters, the microlens will be designed as a stand-alone lens with 0° field. The initial design is done in ZEMAX<sup>®</sup>. Variables are placed on the radius of curvature and conic constant. The design is then optimized for spot size, resulting in a lens with a radius of curvature of 0.407 mm and a conic constant of -2.92. The sag is largest at the corners of the microlens and equal to 35.5  $\mu\text{m}$ . Light will come to a focus 100  $\mu\text{m}$  beyond the last surface with a diffraction limited spot size of 1.73  $\mu\text{m}$  in air (see Fig. 4).

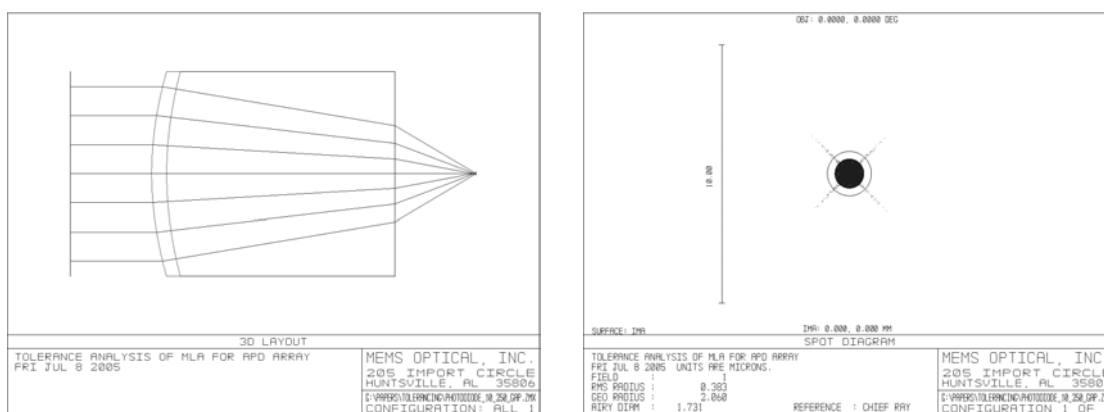


Fig. 4. Layout of the optical system for a single pixel (left) with a spot diagram (right).

Copyright 2006 Society of Photo-Optical Instrumentation Engineers. This paper will be published in SPIE Proceedings Micromachining and Technology for Micro-Optics and Nano-Optics IV and is made available as an electronic preprint with permission of SPIE. One print or electronic copy may be made for personal use only. Systematic or multiple reproduction, distribution to multiple locations via electronic or other means, duplication of any material in this paper for a fee or for commercial purposes, or modification of the content of the paper are prohibited.

Using equations 7 and 8 and assuming a  $\pm 5\%$  etch uniformity, the maximum and minimum values for radius of curvature and conic constant were found. The specific amounts were then verified and altered if necessary by equation 4. The results are summarized in Table 1. Again, wafer thickness and index of refraction have been assumed to be constant. The range of conic values given in Table 1 may require some explanation. An optical engineer with classical optics training might conclude that the process is not very well controlled. That the conic constant can vary by nearly 50% of its nominal value implies that there is no ability to control the lens shape in grayscale lithography. After all, the only difference between a spherical lens and a parabolic lens is one conic unit. Nevertheless, it would be best to keep in mind that the maximum radial aperture of the lens is a mere  $177\mu\text{m}$  and the change in sag represents only 5% of the maximum. It would be a more accurate statement to say that there is little difference in the lens shape over this range of conic values as can be seen in Figure 5.

Table 1. Tolerance values used in the analysis (all units are in millimeters).

Parameter	Nominal value	Minimum value	Maximum value
<i>Radius of curvature</i>	0.407046	0.384236	0.43209
<i>Conic constant</i>	-2.92176	-4.41489	-1.69197
<i>Wafer thickness</i>	0.300	0.300	0.300
<i>Index of refraction</i>	3.105	3.105	3.105

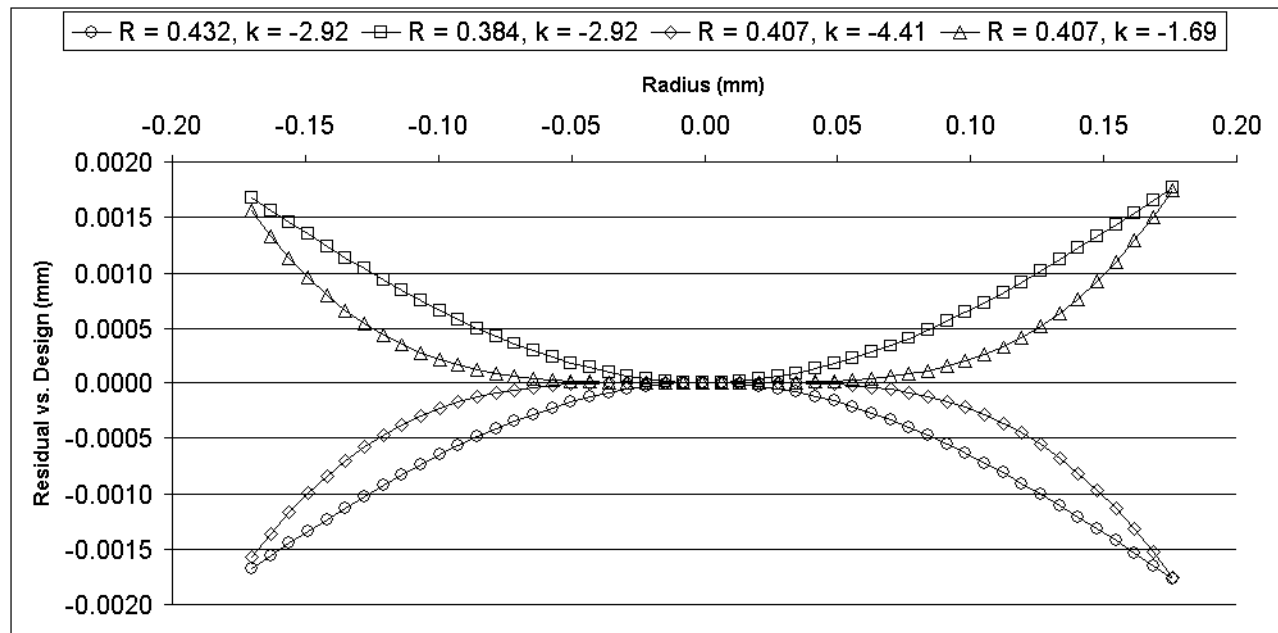


Fig. 5. Deviation of the sag from design across the microlens aperture.

Figure 6 provides the spot size of the lens in microns as a function of radius of curvature and conic constant. It should be noted that the contour lines trace ellipses in the design space. This result makes sense if one considers that the optical performance criterion is spot size. Spot size is strongly affected by focal length, and the focal length is directly related to the curvature of the lens surface. If the radius of curvature were to increase, the lens would flatten out, decreasing the curvature and increasing the spot size. However, if the conic constant were to increase as well, the surface of the lens will curve more steeply at the edges, bending the marginal rays more and decreasing the spot size. Figure 7 shows a SEM image of a microlens fabricated in GaP using grayscale technology. The fabricated lens parameters are similar to those listed above.

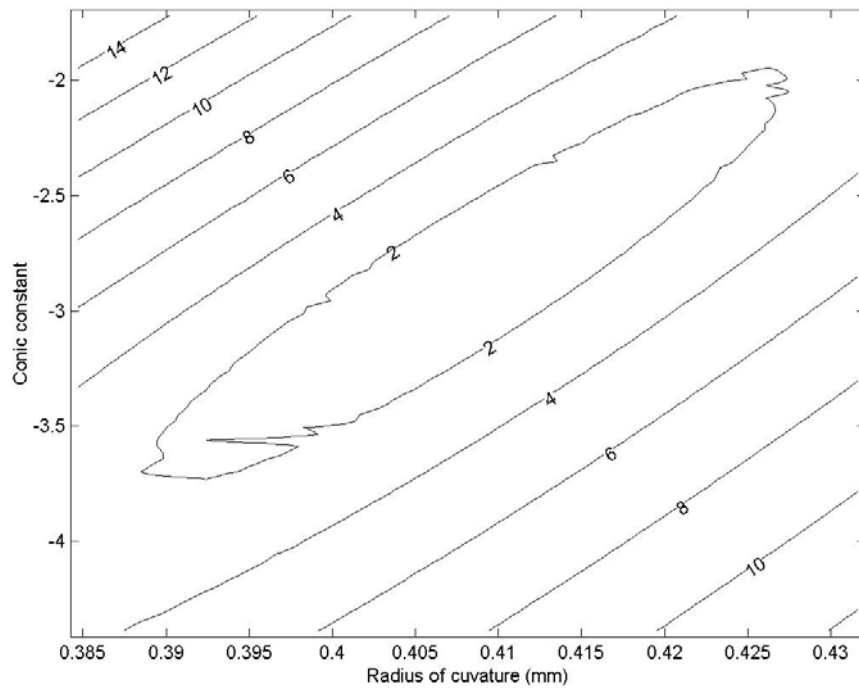


Fig. 6. Contour plot of spot size (in  $\mu\text{m}$ ) for tolerance on radius of curvature and conic constant.

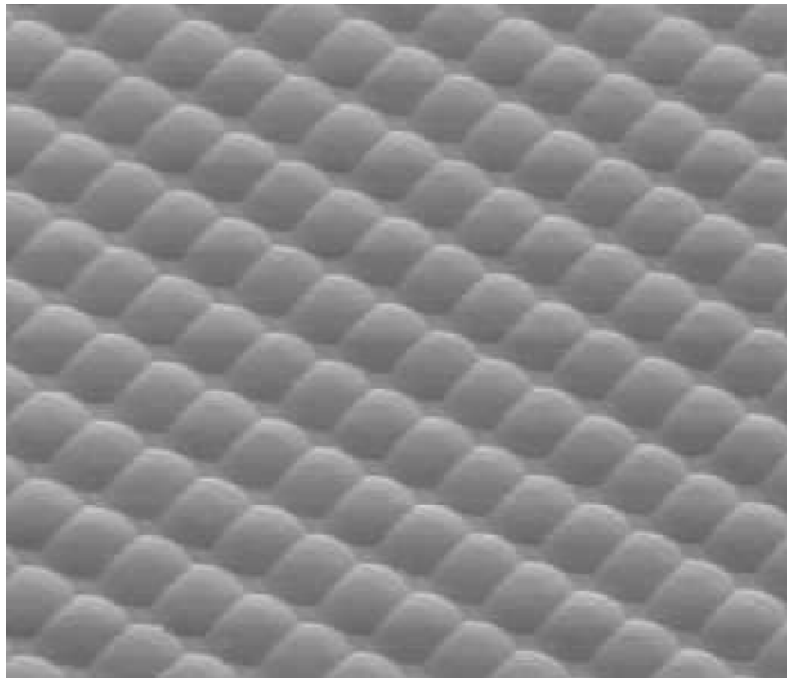
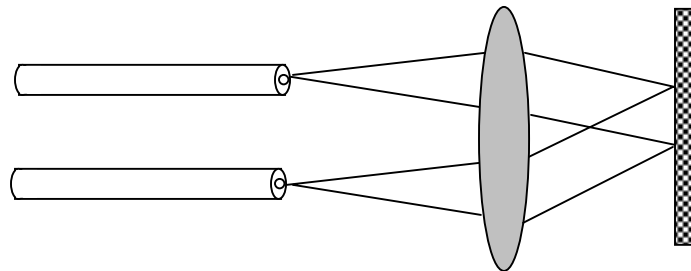


Fig. 7. SEM image of a microlens fabricated in GaP using grayscale technology.

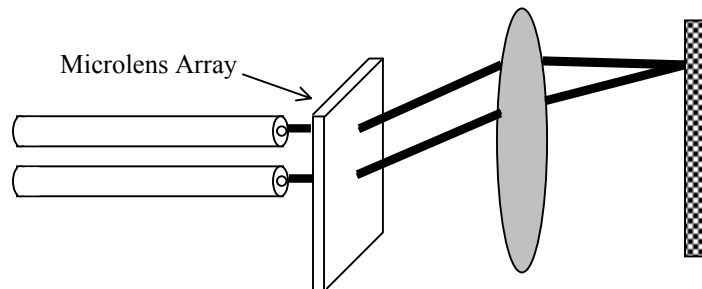
Copyright 2006 Society of Photo-Optical Instrumentation Engineers. This paper will be published in SPIE Proceedings Micromachining and Technology for Micro-Optics and Nano-Optics IV and is made available as an electronic preprint with permission of SPIE. One print or electronic copy may be made for personal use only. Systematic or multiple reproduction, distribution to multiple locations via electronic or other means, duplication of any material in this paper for a fee or for commercial purposes, or modification of the content of the paper are prohibited.

#### 4. FIBER COUPLING

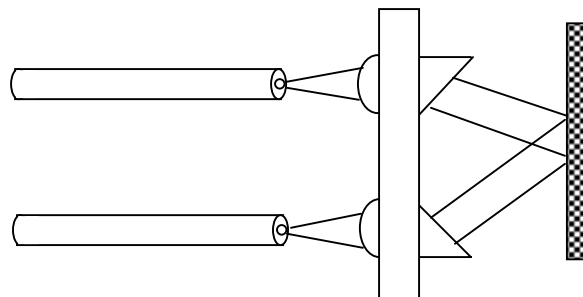
In this section, biconic microlenses are modeled for potential use in optical switching applications. Optical switching with  $1 \times N$  or  $2 \times N$  fiber arrays can be achieved with an optical system consisting of macro optical elements of lenses and scanning mirrors.<sup>6</sup> Implementing micro-optics such as MEMS mirrors and microlens arrays reduces size and longitudinal tolerance requirements. Figure 8 shows some of these concepts. Configurations having all micro-optical components as shown in Figure 8(c) allow for steering and coupling with less mechanical components. The alignment tolerances are reduced due to two optical functions being produced as a monolithic component. Double-sided optics incur additional cost due to the extra processing steps and mask costs. Biconic microlenses can be manufactured in a single photolithography step using grayscale technology enabling the ability to steer light and couple effectively without additional mechanical or optical components.



(a) Macro optical approach to optical switching.



(b) Microlens array shifted vertically.



(c) Microlens array and micro-prism structures for steering.

Fig. 8. Concepts for optical switching.

Figure 9 shows the solid model for a biconic design. The physical optics propagation (POP) model within ZEMAX<sup>®</sup> was used to determine the coupling efficiency. The input waist parameters for POP are defined at the  $1/e^2$  points for a Gaussian beam, which differs from the specifications published by Corning<sup>®</sup> for the SMF-28<sup>™</sup> fiber.<sup>7</sup> Corning specifies the numerical aperture at 1% of the peak intensity of a Gaussian beam. A numerical aperture of 0.09 is calculated at the  $1/e^2$  points. The input and output fibers for the POP analysis are defined with an NA of 0.09 with waist at the mode field diameter for 1550nm. The nominal coupling efficiency is 99% for the biconic design based on the POP model for a single-mode fiber.

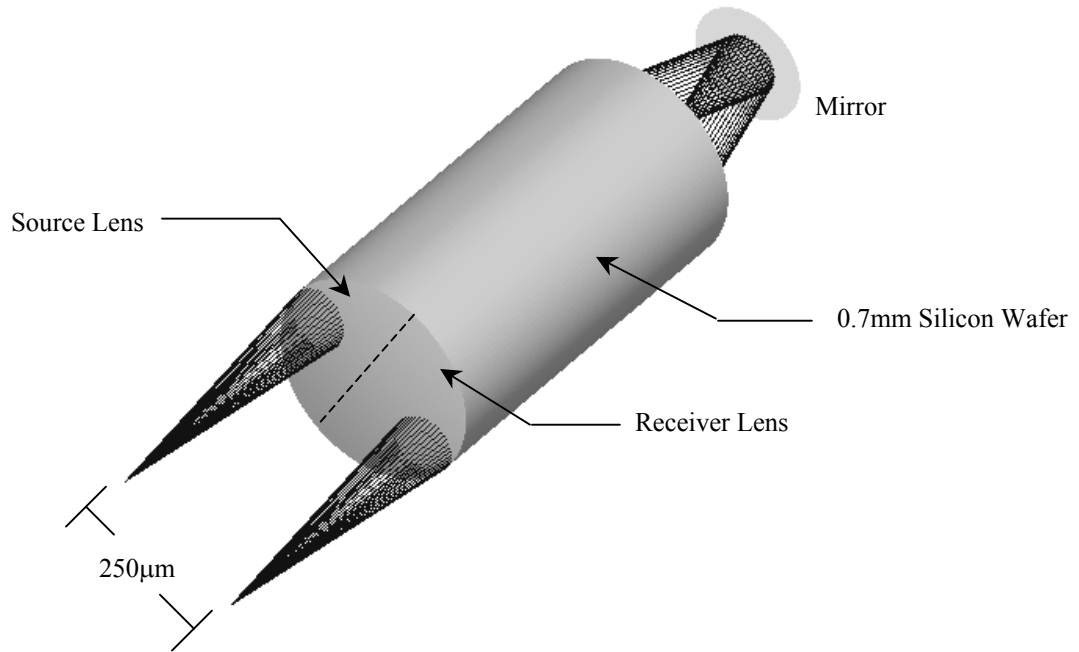


Fig. 9. Solid model of biconic design.

Figure 10 shows the 2D layout of the unfolded system used to perform the tolerance analysis. The biconic design is valuable in correcting coma and astigmatism, which are aberrations resulting from having off-axis ray bundles. The biconic design also compensates for having a non-symmetric entrance pupil. The disadvantage of the biconic design is the additional radius of curvature (RoC) and conic tolerances for each dimension, X and Y in contrast to a symmetrical design having only a single RoC and conic tolerance. Figures 11 and 12 provide the tolerance metrics for  $RoC_x$  versus  $RoC_y$  and  $conic_x$  versus  $conic_y$ , respectively for the biconic design.

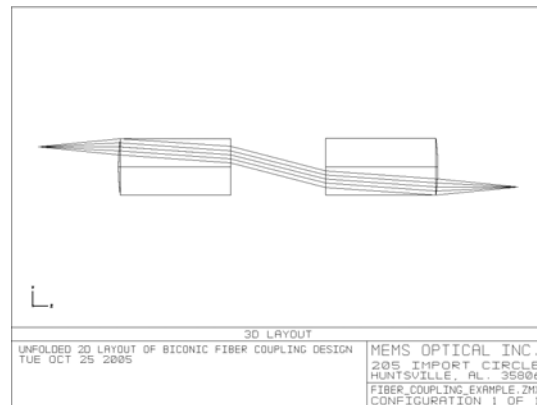


Figure 10. 2D layout of unfolded biconic design for tolerancing.

Copyright 2006 Society of Photo-Optical Instrumentation Engineers. This paper will be published in SPIE Proceedings Micromachining and Technology for Micro-Optics and Nano-Optics IV and is made available as an electronic preprint with permission of SPIE. One print or electronic copy may be made for personal use only. Systematic or multiple reproduction, distribution to multiple locations via electronic or other means, duplication of any material in this paper for a fee or for commercial purposes, or modification of the content of the paper are prohibited.

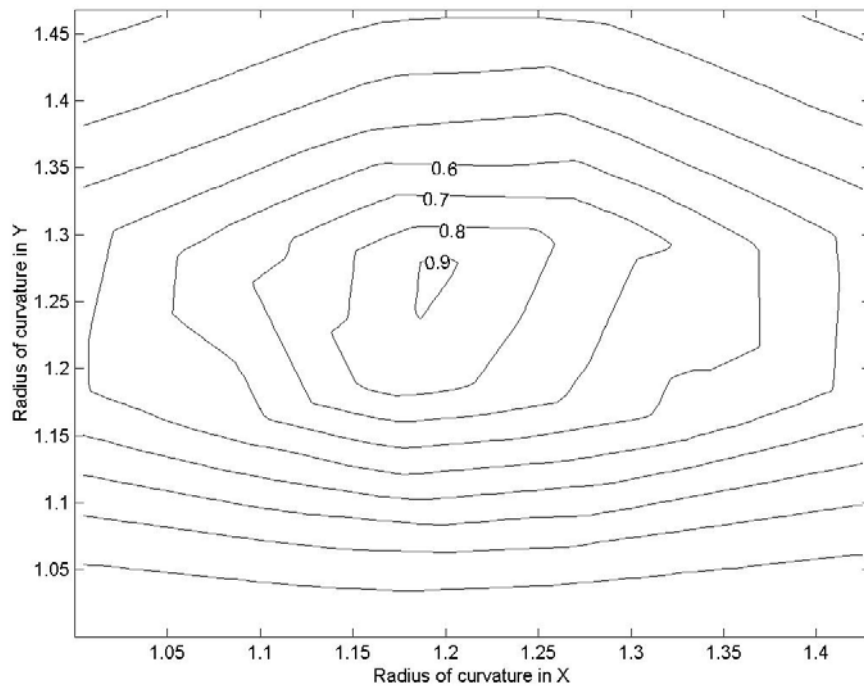


Fig. 11. Contour plot of coupling efficiency for tolerance on  $RoC_y$  and  $RoC_x$ .

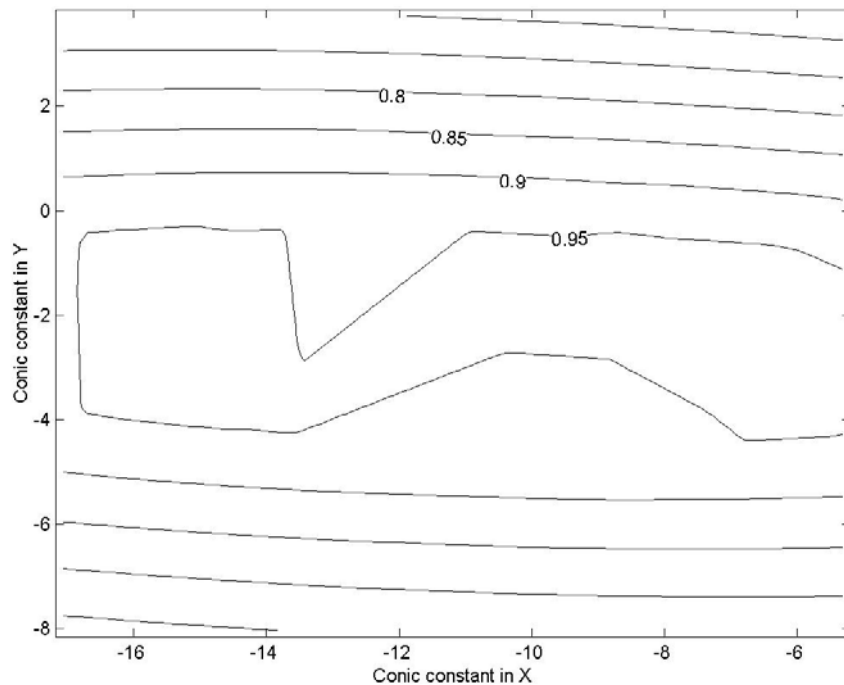


Fig. 12. Contour plot of coupling efficiency for tolerance on  $conic_y$  and  $conic_x$ .

The RoC tolerance metric shows that approximately a  $\pm 4\%$  change in  $\text{RoC}_y$  and approximately a  $\pm 6\%$  change in  $\text{RoC}_x$  yield greater than 70% coupling efficiency. The conic tolerance metric shows that approximately a  $\pm 6$  change in conic units in either direction still yield greater than 70% coupling efficiency. The RoC tolerance metric is for the most part radially symmetric mainly due to the fact that the nominal values for RoC in each direction are approximately equal. The conic tolerance metric shows that to maintain a higher coupling efficiency the conic in the Y dimension must be maintained to approximately  $\pm 2$  conic units for  $>90\%$  coupling. Figures 13 and 14 are tolerance results for RoC and conic in each dimension independently and take on the expected elliptical nature as previously shown in Figure 6. Fiber coupling efficiency is similar to designing for a small spot in that aberration correction is key to both instances. The tolerance metrics show that as the RoC increases resulting in less sag that the conic must also increase to maintain the same performance. Figure 14 shows that the variation in the Y direction is the most sensitive due to the larger aperture size in this dimension. Having the ability to view the change in radius of curvature and conic constant over a wide range of values allows the design and fabrication groups to determine the sensitivity and manufacturability of the microlens.

In doing the fiber coupling tolerance, none of the alignment tolerances for the cladding-to-core-concentricity, fiber-to-fiber pitch, or lens-to-fiber spacing were considered in the analysis. The tolerance routine within ZEMAX<sup>®</sup> allows for such parameters to be included; however, the focus of the analysis is on microlens manufacturing using grayscale technology. Others have reported that tilts, lateral shifts, and longitudinal shifts can contribute an additional 0.25-1dB loss. Systems have been reported as much more sensitive to longitudinal misalignments in which the fibers are cleaved at an  $8^\circ$  angle to minimize return loss when there is an air gap between the fiber and the lens<sup>8</sup>. The eccentricity of the core of the fiber and the fiber positioning within a bundle or array has also been reported to cause an additional 1dB loss.<sup>6</sup> The alignment, fiber, and lens tolerances can all add up to result in a coupling loss between -3dB and -2dB.

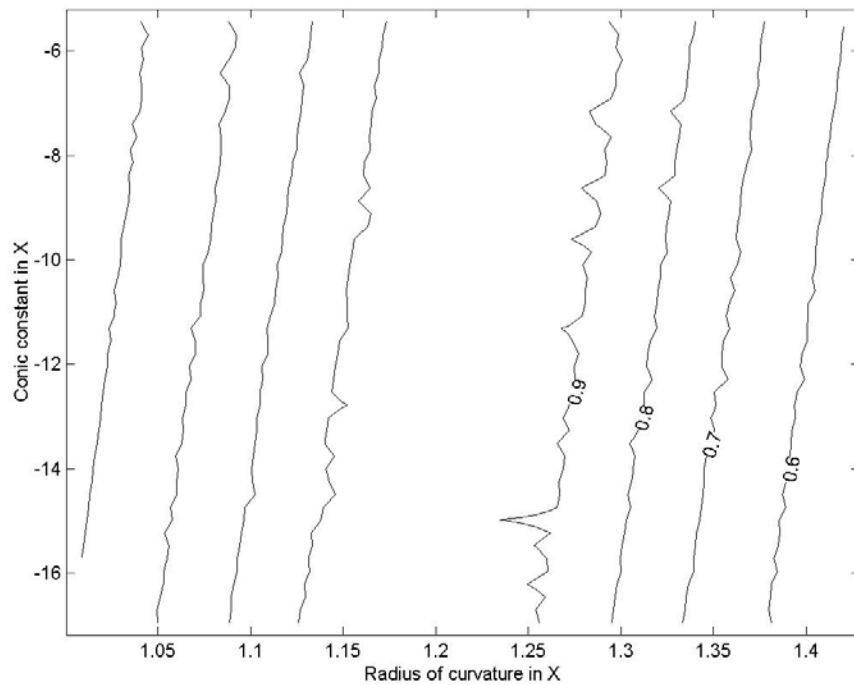


Fig. 13. Contour plot of coupling efficiency for  $\text{RoC}_x$  and  $\text{conic}_x$ .

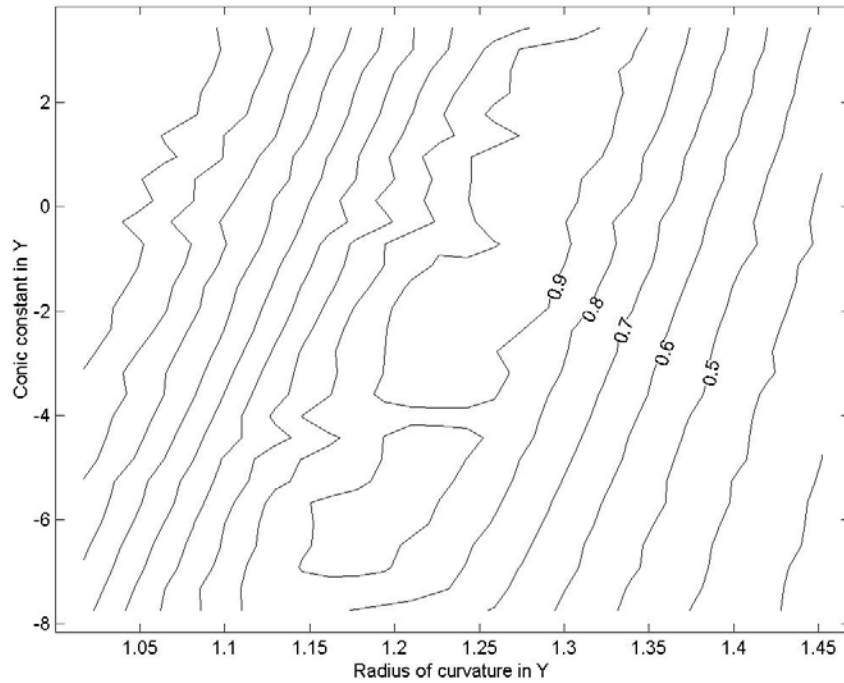


Fig. 14. Contour plot of coupling efficiency for  $RoC_y$  and  $conic_y$ .

Figure 15 shows a SEM image of an off-axis microlens array for a similar fiber coupling application. An individual lens has dimensions of  $250\mu\text{m} \times 695\mu\text{m}$  with a maximum sag of  $41\mu\text{m}$ . The vertex of the lens is shifted by  $103\mu\text{m}$  from the center of the lens aperture in the X dimension.

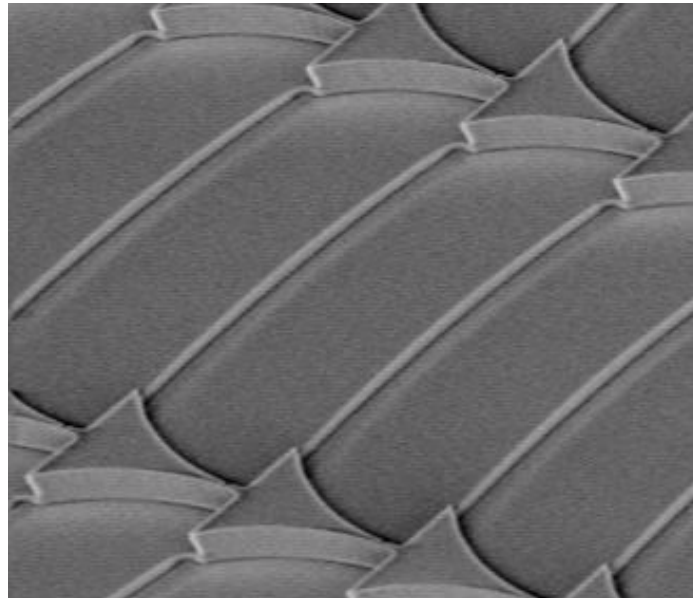


Fig. 15. SEM image of off-axis lenses fabricated in fused silica for a fiber coupling application.

Copyright 2006 Society of Photo-Optical Instrumentation Engineers. This paper will be published in SPIE Proceedings Micromachining and Technology for Micro-Optics and Nano-Optics IV and is made available as an electronic preprint with permission of SPIE. One print or electronic copy may be made for personal use only. Systematic or multiple reproduction, distribution to multiple locations via electronic or other means, duplication of any material in this paper for a fee or for commercial purposes, or modification of the content of the paper are prohibited.

## 5. SUMMARY

A new tolerance technique is needed for microlenses fabricated using grayscale technology. Applying a tolerance to one parameter while holding all other parameters fixed relies on the assumption that the parameters are independent of one another, which is not always true. In the equation for the sag of a lens, for instance, the radius of curvature and conic constant are coupled. Thus, the measured values for radius of curvature and conic constant can lie anywhere in the two-dimensional space defined by the change in sag resulting from etch uniformities. If the change in sag is a random process, it becomes important to map the full two-dimensional space and using the Monte Carlo method in ZEMAX<sup>®</sup> is the easiest way to do this. Displayed graphically, the affect on optical performance of tolerancing any two design parameters can be shown. A technician can map the measured lens onto the design space with a few keystrokes and immediately see if the lens will give acceptable performance. By automating the measurements an entire wafer containing thousands of lenses can be analyzed quickly and regions on the wafer that will yield good parts can be identified (see Fig. 16).

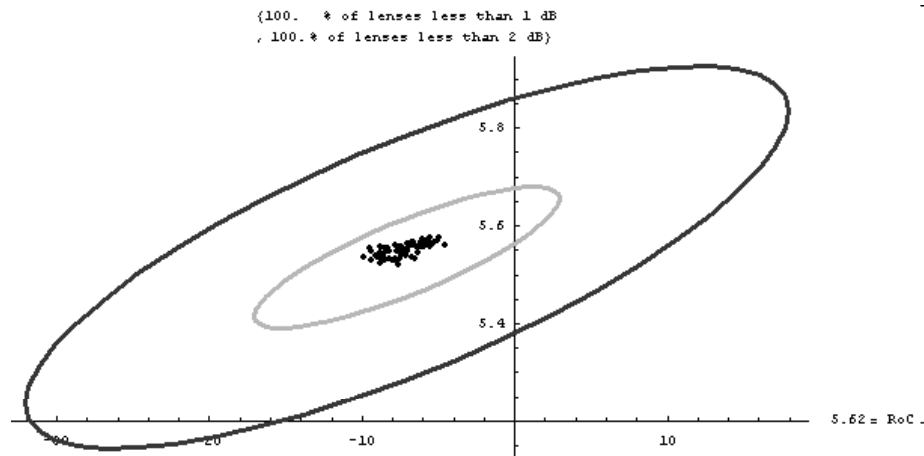


Fig. 16. Scatter plot of RoC and conic values for fiber-coupling microlenses (the smaller ellipse represents 1dB loss).

## REFERENCES

1. P. Foote and R. Woodson, "Lens design and tolerance analysis methods and results," *J. Optical Society of America* **38**, 590-599, 1948.
2. M. R. Wang and H. Su, "Laser direct-write gray-level mask and one-step etching for diffractive microlens fabrication," *Applied Optics* **37**, 7568-7576, 1998.
3. T. Pandhumsoporn, et al., "High etch rate, deep anisotropic plasma etching of silicon for MEMS fabrication," [http://www.adixen.com/adixen\\_avt/download/docs/news/doc119.pdf](http://www.adixen.com/adixen_avt/download/docs/news/doc119.pdf), October 2005.
4. J. D. Strasburg, T. W. Murphy Jr., E. G. Adelberger, C. W. Stubbs, D. W. Miller, and J. I. Angle, "The advantages of avalanche photodiode (APD) arrays in laser ranging applications," 13th International Laser Ranging Workshop, Washington, D. C., USA, 2002.
5. B. Aull, et al., "Geiger-Mode Avalanche Photodiodes for Three-Dimensional Imaging", [http://physics.ucsd.edu/~tmurphy/apollo/doc/Aull\\_LLJ.pdf](http://physics.ucsd.edu/~tmurphy/apollo/doc/Aull_LLJ.pdf), October 2005.
6. Y. Peter, "Micro-optical fiber switch for a large number of interconnects," M.S. Thesis, Université de Neuchâtel Institut de Microtechnique, Jan. 2001.
7. Corning<sup>®</sup> SMF-28<sup>™</sup> Optical Fiber Product Information Issued April 2002. <http://www.ee.byu.edu/photonics/connectors.parts/smf28.pdf>, October 2005.
8. Shiefman, J, "Insertion loss comparison of microcollimators used to propagate light in and out of single mode fibers," *Optical Engineering* **43**, 1927-1937, 2004.

Copyright 2006 Society of Photo-Optical Instrumentation Engineers. This paper will be published in SPIE Proceedings Micromachining and Technology for Micro-Optics and Nano-Optics IV and is made available as an electronic preprint with permission of SPIE. One print or electronic copy may be made for personal use only. Systematic or multiple reproduction, distribution to multiple locations via electronic or other means, duplication of any material in this paper for a fee or for commercial purposes, or modification of the content of the paper are prohibited.